Age-related differences in brain activations during spatial memory formation in a virtual Morris water maze task

by
Nadjalisse C. Reynolds-Lallement

A THESIS

Submitted to

Oregon State University

Honors College

In partial fulfillment of
the requirements for the
degree of

Honors Baccalaureate of Science in Biochemistry & Molecular Biology
(Honors Scholar)

Presented May 25, 2018
Commencement June 2018

AN ABSTRACT OF THE THESIS OF

Nadjalisse Reynolds-Lallement for the degree of Honors Baccalaureate of Science in Biochemistry & Molecular Biology presented on May 25, 2018. Title: Age-related differences in brain activations during spatial memory formation in a virtual Morris water maze task.

Abstract approved: _____

Kathy Magnusson

This study applied a virtual rendition of the Morris water maze, which is commonly used for assessing spatial memory in rodents, to an examination of age-related differences in spatial learning among 42 younger (18-30 years) and older (>60 years) male human participants. Virtual Morris water maze performance was measured by cumulative proximity to the goal corrected for start position across 44 learning trials. After controlling for age differences in visible trial pathlength, older adults exhibited greater cumulative proximity to the goal than younger adults. When older participants were categorized into good and poor performers based on a median split of their performance across hidden trials, poor older performers searched away from the hidden platform more than young adults. fMRI scanning was conducted during the final, well-learned phase of water maze trials. Greater activation was witnessed in young adults in the cerebellum compared to older adults, and older good performers displayed greater activation in the middle and superior frontal gyrus than older poor performers. These findings suggest that older adults may be poorer at acquiring spatial memories and show functional differences when performing spatial memory tasks, calling for further investigation into the neural mechanisms of age-related differences in spatial memory formation.

Key Words: spatial memory, fMRI, Morris water maze, cognitive aging, navigation

Corresponding e-mail address: nadjalisse.reynolds@gmail.com

Age-related differences in brain activations during spatial memory formation in a virtual Morris water maze task

by
Nadjalisse Reynolds-Lallement

A THESIS

Submitted to

Oregon State University

Honors College

In partial fulfillment of
The requirements for the
Degree of

Honors Baccalaureate of Science in Biochemistry & Molecular Biology
(Honors Scholar)

Presented May 25, 2018
Commencement June 2018

Honors Baccalaureate of Science in Biochemistry & Molecular Biology project of Nadjalisse Reynolds-Lallement presented on May 25, 2018

APPROVED:

Kathy Magnusson, Mentor, representing Department of Biomedical Sciences

Fikru Nigussie, Committee Member, representing Department of Biomedical Sciences

Anita Cservenka, Committee Member, representing Department of Psychology

Toni Doolen, Dean, Oregon State University Honors College

I understand that my project will become part of the permanent collection of Oregon State University, Honors College. My signature below authorizes release of my project to any reader upon request.

Nadjalisse Reynolds-Lallement, Author

TABLE OF CONTENTS

Page

LIST OF FIGURES AND TABLES

Page

FIGURES

TABLES

1. INTRODUCTION

The population of the United States is aging, and with an aging population come increased health consequences associated with age-related memory decline. Loss of memory can be emotionally devastating to families, financially burdensome to society, and severely inhibit independence and quality of life for a significant portion of the population. One of the cognitive effects of aging is impaired spatial memory, which is a critical skill for navigating and coping with one's environment (Evans et al., 1984; Cherry & Park, 1993; Kirasic & Bernicki, 1990; Moore et al., 1984; Sharps & Gollin, 1987; Moffat & Resnick, 2002). Impaired spatial navigation ability has been proposed to be a cognitive indicator of early Alzheimer's disease (Benke et al., 2014; Lithfous et al., 2013; Vlcek & Laczo, 2014), thus increasingly it is necessary to characterize the neural mechanisms that underlie age-related changes in spatial memory.

The Morris water maze (MWM) is a sensitive, commonly used assessment of spatial learning and memory. In the MWM, which was originally designed to assess place navigation in rodents, a test subject learns over repeated trials the location of a hidden platform in a controlled environment using fixed spatial cues (Morris, 1981). The protocol has been refined by multiple researchers since its conception (Morris, 1984; Vorhees & Williams, 2006) and is considered the "gold standard" for evaluating spatial memory formation. Due to its sensitivity, the MWM has been used to establish a rodent model of age-related memory decline (Begega et al., 2001; Gallagher & Pelleymounter, 1988; Lindner et al., 1997; Lukoyanov et al., 1999; Magnusson et al., 2007). Many of these models focus on the importance of the hippocampus in coordinating spatial memory formation (Morris et al., 1982). For example, Knierim et al. (1995) found that specialized place cells in the hippocampus respond to specific locations, and this response changes with age.

To create a cross-species understanding of the functional and behavioral mechanisms underlying cognitive aging, it is necessary to use assessments and measurements that are closely aligned with those used to study cognition in animals. Virtual navigation tasks are well-equipped to detect age-related differences in spatial memory. Waller et al. (1998) found that a virtual environment is adequate for evaluating real-life spatial learning ability. Virtual environments have been used to assess human navigation (Maguire et al., 1999; Van Veen et al., 1998) and acquisition of spatial knowledge (Gillner & Mallot, 1998; Moffat et al., 2001). Virtual environments have also been used in neuroimaging studies (Aguirre & D'Esposito, 1996; Gron et al., 2000). Virtual environment testing can be advantageous over traditional behavioral tests because the researcher can have complete control over the subject's environment. Additionally, the effects of confounding variables such as age-related differences in motor skills are decreased, and the task can be conducted in a confined environment such as a magnetic resonance imaging scanner.

The MWM has been adapted for human use by creating virtual reality translations for cross-species assessment of spatial learning (Astur et al., 1998; Moffat & Resnick, 2002; Rahman et al., 2008; Zhong et al., 2017). There is evidence that using the MWM with rodents and a virtual Morris Water Maze (vMWM) in humans yields consistent and sensitive results across species (Schoenfeld et al., 2017; Possin et al., 2016). Previous vMWM studies have characterized age differences in spatial knowledge acquisition. Moffat & Resnick (2002)

demonstrated that older participants show spatial memory deficits in a vMWM, and this effect may be partially due to deficiencies in allocentric mapping. Newman & Kaszniak (2000) and Daugherty & Raz (2017) to found that older adults show deficits in place navigation compared to young, and Laurance et al. (2002) showed that older adults form and recall accurate cognitive maps in a vMWM but fail to recall locations within the map.

There is considerable evidence that, in addition to the hippocampus, the prefrontal cortex plays an influential role in spatial memory and learning ability (Jo et al., 2007; Lee & Kesner, 2003; Yoon et al., 2008; Preston & Eichenbaum, 2013; Martinet et al., 2011; Kessels et al., 2000; Sapiurka et al., 2016; Touzani et al., 2007; Pratt & Mizumori, 2001). Moffat et al. (2006) showed that during virtual spatial navigation, older humans showed reductions in activation in hippocampus and parahippocampal gyrus, but increased activation in anterior cingulate gyrus and medial frontal lobe, compared to young subjects. Additionally, Moffat et al. (2007) found that increased virtual navigation ability was associated with larger volume of prefrontal gray and white matter. To date, it remains unclear if the recruitment of additional neural resources by older individuals when completing the same task as younger individuals is a useful compensation for age-related deficits or a product of age-related dedifferentiation or decreased ability to use specialized neural mechanisms (Reuter-Lorenz & Cappell, 2008; Cabeza, 2001). This study lays the groundwork for investigating the recruitment of extrahippocampal regions, such as the prefrontal cortex, and its role in spatial learning and memory in older adults.

This study utilized a vMWM that was designed to closely match the rodent MWM protocol from Magnusson et al. (1998, 2007) and Zhao et al. (2009). The design and specifications of this vMWM are described previously in detail (Zhong et al., 2017). We hypothesized that this new virtual water maze task would be sensitive to age-related changes in spatial learning in humans, and these changes would be associated with differences in brain activation between older adults vs. young adults during a well-rehearsed phase of the task. We hypothesized that older adults would show impaired spatial memory, when tested over multiple trials, as compared to young adults in a vMWM. More specifically, we predicted that increased activations in the prefrontal cortex would underlie impaired spatial memory in older humans, as seen in mice (Magnusson et al., 2007, Moffat et al., 2007).

This study provides a translational model for examining age-related declines in spatial memory and underlying brain response in older adults. Evidence of age-related spatial memory decline using a translational model may help pave the way for animal behaviorists to translate their research to humans and test interventions into cognitive aging and dementia.

2. METHODS

2.1 Participants

21 younger (ages 18-30, mean = 22.3, *SD* = 3.1) and 21 older adult males (ages 60-79, mean = 65.7, *SD* = 4.5) were used in this study. All participants were male due to documentation of sex differences in human vMWM performance (Astur et al., 1998; Daugherty et al., 2015; Driscoll et al., 2003; Nowak et al., 2014). Young adults were recruited from the Georgia Institute of Technology research volunteer pool. Older adults were recruited from the Atlanta community using newspaper advertisements and notices posted at adult community centers. The study was approved by the Georgia Institute of Technology Institutional Review Board, and written informed consent was obtained from each participant.

All participants were right-handed as assessed by the Edinburgh handedness questionnaire (Oldfield, 1971). Based on self-reported medical history, participants were excluded if they had a current diagnosis or history of coronary heart disease, stroke, diabetes, high blood pressure, or dementia. None of the participants took medications that could affect cognition. Participants completed the Mini-Mental State Exam (MMSE) with an exclusion score of $\leq 27/30$ to rule out dementia, and one participant was excluded based on this criterion (Folstein et al., 1975; O'Bryant et al., 2008). Based on the self-report Center for Epidemiologic Studies Depression Scale, all participants had scores below 16, indicating no clinical levels of depression in the current sample that could affect daily functioning. Participants had 20/40 visual acuity or better, normal color vision as judged from the Ishihara Color Plates Test, and normal contrast sensitivity based on the Mars Letter Contrast Sensitivity Test.

2.2 Procedures

2.2.1 vMWM and Pre-Task Training

The vMWM was designed using SketchUp Pro, 2014 (Trimble Navigation Ltd., Sunyvale, CA) and Unity Pro 5.0.2 (Unity Technologies, Inc., San Francisco, CA). Participants sat approximately 30 cm in front of a 21-inch, flat-panel LCD monitor at eye level when performing the vMWM. Before beginning the experiment, participants explored a separate arena by navigating to four objects (a car, a bench, a tree, and a chair) located in the four corners of the arena. Next, they completed a joystick control speed test in a separate virtual maze (designed using Unreal Engine v3.0; Epic games, Inc., Cary, NC). Younger (M = 57s, *SD* = 4.7) and older (M = 64s, *SD* = 15.3) participants finished the maze by reaching a flagged finishing point in a similar time frame, demonstrating satisfactory joystick control ($p < 0.05$).

Participants next practiced looking for a hidden platform located in a circular pool of water in a non-testing vMWM using object cues. The test vMWM was scaled to the 3D dimensions of the real-world rodent MWM used by Magnusson *et al.*, 2007 (Fig. 1A). Four black object cues of the same size (square, star, triangle, circle) were located high on the arena walls. The corners of the arena were curved to prevent them being used as visual cues. A hidden platform (1.4% of the pool's surface area) had a fixed location in the middle of the pool's southeast quadrant.

2.2.2 Experimental Testing

2.2.2.1 Initial (out of scanner) testing (A1)

Participants completed 27 trials in the vMWM in which they were instructed to navigate to the hidden platform as efficiently as possible (Fig. 1A, 2A-C). The trial sequence consisted of 24 hidden-platform place trials (60 s maximum swim time) and 3 probe trials (30 s maximum swim time) with the platform absent: one naïve probe trial at the beginning, the second probe after 12 place trials, and the third probe trial at the end of place trials. Entry points were systematically varied among the NW, NE, and SW quadrants. Subjects first completed the 30-second naïve probe trial in the vMWM with the platform absent, in which they were told to explore the arena and no platform would be present. Participants were not told that there would be any more platform-absent probe trials or whether the platform would be stationary across place trials, because mice in the traditional MWM also lack this foreknowledge. When subjects reached the location of the hidden platform during place trials, the platform became visible to them on the pool's surface (Fig. 2C). Participants had 5s between trials during which they could rotate using the joystick but could not leave the platform. If subjects did not find the platform location within the maximum trial time (60s), a movie played on the screen that guided them to the platform, and they were still given 5s to rotate on the platform.

Following the third probe trial, participants performed 6 visible-platform control trials to control for learning-independent factors such as motivation, visuomotor ability, and navigation ability. The arena used in the control trials was a round pool with no differentiating environmental cues (Fig. 1B). The same platform was used, but it was visible on the pool's surface and highlighted with a dome of yellow light (Fig. 2E). The location of the platform systematically varied between all four quadrants and the center of the pool, and entry points varied between N, S, E, and W. Participants were instructed to navigate as efficiently as possible to the platform in each trial as before.

2.2.2.2 Mock scanner (A2) & fMRI scanner (A3) testing

Next, participants completed 4 hidden and 6 visible trials interleaved in a mock fMRI scanner (MRI simulator^{TM}, Psychology Software Tools, Sharpsburg, PA) to practice doing the task in the confined, noisy environment of an fMRI scanner. To enhance the likelihood of participants engaging memory processes in the scanner, at the beginning of the mock scanner trials, they were told that the platform was stationary and would remain in the same location as in previous trials. Finally, participants completed 16 hidden and 8 visible trials interleaved in an fMRI scanner. The task was considered well-learned at this time. The maximum time allowed for hidden trials in the mock and fMRI scanners was 30s.

A. B.

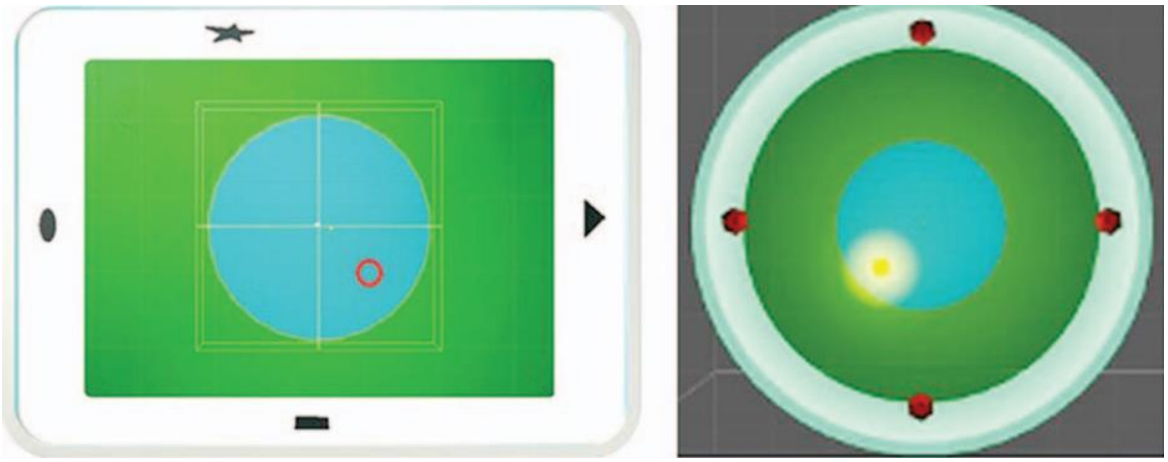

Figure 1: Overhead views of (A) the vMWM arena used for hidden and probe trials and (B) the arena used for visible/control trials. (A) Four black-and-white shape cues were placed high up on the wall. The location of the platform in the SE quadrant is indicated with a red circle. (B) Four identical red diamonds were placed on the rounded walls to create a uniform environment. Participants navigated to a visible red platform illuminated by a yellow light.

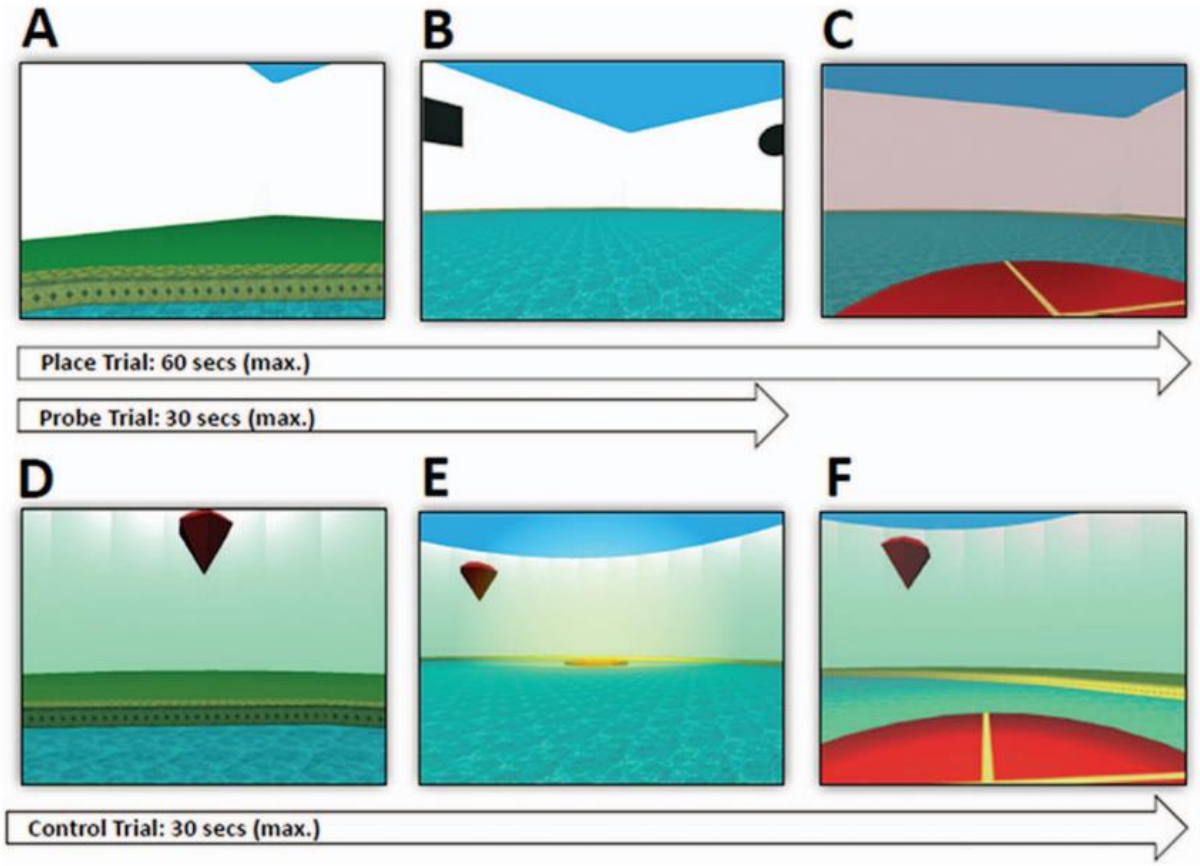

Figure 2: Images of the vMWM arenas used for place (hidden) and probe trials (A-C) and control (visible) trials (D-F) as seen from a participant's point of view. In the experimental vMWM, participants began each trial facing the wall of a circular pool (A) and then use a joystick to explore the pool based on black-and-white shape cues located high up on the walls (B). When the subject arrived at the platform location, it became visible (C) and the participant could rotate in place for 5s. The visible trial arena was similar but designed to have no differentiating environmental cues (D). Subjects navigated with the joystick as quickly as possible to the visible platform illuminated by a yellow light (E-F).
[Source: Fig. 2 from Zhong et al. (2017). Reproduced with permission.]

2.2.3 fMRI Scanning

2.2.3.1 Image Acquisition

Brain images were collected at the Georgia State / Georgia Institute of Technology Center for Advanced Brain Imaging on a 3 Tesla Siemens TIM Trio Magnetic Resonance Imaging system (Siemens Medical Solutions, Erlangen, Germany) with a 12-channel headcoil. Whole-brain structural images were collected in the sagittal plane using a T1-weighted high-resolution MPRAGE scanning sequence (TI = 900 ms, TR = 2250 ms, TE = 4.18 ms, field of view = 256 mm, voxel size = 1.0 mm x 1.0 mm x 1.0 mm, flip angle = 9°, slice thickness = 1.00 mm, 176 slices). Functional images were collected in the transverse plane using a high-resolution

gradient echo-pulse BOLD interleaved slice sequence. (TI = 900 ms, TR = 2250 ms, TE = 4.18 ms, field of view = 256 mm, voxel size = 1.0 mm x 1.0 mm x 1.0 mm, flip angle = 9°, slice thickness = 1.00 mm, 176 slices).

2.2.3.2 Single-Subject Data Preprocessing

fMRI data for all participants were processed and analyzed using the *Analysis of Functional Neuroimages (AFNI)* software package [National Institute of Mental Health, National Institutes of Health; available at: https://afni.nimh.nih.gov/download)]. The acquired brain images/volumes were first corrected for slice timing correction and realigned to the first image. Motion correction followed by registering (i.e., realigning and unwrapping) the BOLD images to the average time-shifted image/volume in each run to correct for image distortions caused by susceptibility-by-movement interactions (Andersson et al., 2001). Fourier interpolation was applied to the heptic degree over two passes to reduce the voxel intensity differences between images to the smallest extent. Subsequently, the high-resolution T1 structural image from each participant was co-registered to the mean BOLD image created from slice timing correction and motion correction using AFNI's "align_epi_anat.py" script. After obtaining these co-registered structural and BOLD images, they were spatially normalized into standard Montreal Neurological (MNI) space, and resampled during normalization to 2 mm^3 isotropic voxels, using AFNI's "@auto_tlrc" program. The structural images of old and young participants were averaged after normalization to act as underlays for the displaying overlays of functional data of old and young participants, respectively. For the display of overlays of functional data comparing the age groups, the structural images of all participants were averaged after normalization to act as the underlay.

To identify task-related changes in the BOLD signal, the time courses of the place/hidden and control/visible trials was examined through a whole-brain analysis. The predicted hemodynamic response for each block of these two types of trials was modeled based on a duration modulated response function as part of AFNI's "3dDeconvolve" program. Timing information about trial onsets and duration in both trial types/blocks was entered as task regressors in the general linear model (GLM). These two regressors were accompanied by six motion regressors-of-no-interest that registered noise pertaining to excessive head motion along the three axes/planes (xyz) of rotation and translation, respectively. A general linear test then subtracted the parameter values representing the control/visible condition from those representing the place/hidden condition to generate whole-brain contrast maps that conveyed the BOLD signal changes during hidden platform search. These parameter difference values were converted to percent signal change (PSC) values to ensure standardized comparisons at the group level. These PSC values were corrected for the extraneous effect posed by the autocorrelation of temporal residuals from regression models via AFNI's "3dREML" program.

2.2.3.3 Group-level Random Effects Analysis

With the contrast maps from each participant, random effect analyses using AFNI's "3dttest++" program were conducted to compare the BOLD signal changes between young and older adults, and within each age group (based on one-sample *t*-tests). To control for any extraneous behavioral effect posed by age differences in visuomotor control of the joystick,

mean visible pathlength (i.e., mean pathlength across all control trials experienced during scanning) was entered as a covariate into the regression analysis. To correct for multiple comparisons of activated voxels across the entire search volume, cluster thresholding was conducted using AFNI's "3dClustSim" program based on a 10,000 iteration Monte Carlo simulation of the whole-brain contrast map derived from the group comparison. AFNI's "3dFWHMx" program was used to estimate the spatial autocorrelation function model parameters to generate the random noise cluster fields for the Monte Carlo simulation. Based on the simulation, the minimum number of voxels fulfilling a height/voxel-wise threshold of 0.01 and a cluster-level threshold of 0.05 was determined to be 133 for all random effects analyses.

2.2.4 Behavioral Analysis

Corrected cumulative proximity was used as a measure of vMWM performance for place and visible trials because it has been found to be a more sensitive measure of performance than the traditional latency or pathlength (Gallagher *et al.*, 1993; Maei *et al.*, 2009). Cumulative proximity was calculated as sum of the participant's distances to the platform's center computed every 0.2 ms until the hidden platform was found or the time limit was up (60s for place trials, 30s for probe trials). Cumulative proximity was then corrected for the participant's varying entry locations. Essentially, CCProx is the participant's search error from the "ideal" path to the platform. In both measures of search performance, navigation speed is not as confounding a variable as latency. Mean visible pathlength from A1 or A2 and A3 control trials were used as covariates in the analysis of the respective hidden trials to account for age-related differences in visuomotor control ability.

2.2.5 Median Split

Older adults were separated into good-performing and poor-performing groups based on a median split of their corrected cumulative proximity data over 24 A1 place trials (see Zhong et al., 2017 for details of this procedure). This split resulted in 11 older good-performing (mean age = 66.3, *SD* = 3.6) and 10 older poor-performing participants (mean age = 65.1, *SD* = 5.1) based on a median corrected cumulative proximity of 261.77 (Table 2). The two groups showed no significant differences in age or other demographic information. This median split was used to analyze behavior in A1 place trials, probe trials, and visible trials.

Behavioral results in A2 and A3 were analyzed using a median performance split of older participants based on corrected cumulative proximity data over 20 A2 and A3 place trials. This split once again resulted in 11 older good-performing (mean age = 66.0 *SD* = 3.5) and 10 older poor-performing participants (mean age = 65.4, *SD* = 5.6) based on a median corrected cumulative proximity of 137.33, but the composition of the two older subgroups differed from those calculated based on an A1 median split (Table 3). A median split based on corrected cumulative proximity from A3 trials only resulted in the same categorization of good- vs poor-performing older adults (median = 114.87) as the A2 and A3 split and was used in fMRI data analysis.

3. RESULTS

3.1 Participant characteristics

Younger and older participants demonstrated significant differences in contrast sensitivity and time to complete a pre-task speed test ($p < 0.05$, Table 1). There were no significant differences in participant demographics and characteristics between good-performing and poor-performing older adults divided by a median split in out-of-scanner vMWM performance (Table 2). When divided by median in-scanner vMWM performance, older poor performers required a significantly greater number of trials to demonstrate competency in the practice vMWM than older good performers ($p = 0.03$, Table 3).

Table 1: Participant Demographics and Test Results

	Young (n = 21)			Old (n = 21)			Difference (Old – Young)		
Demographic or pretest variable	M (SD)	Min.	Max.	M (SD)	Min.	Max.	M	95% CI	p-value
Age*	22.29 (3.13)	18	30	65.71 (4.51)	60	79	43.43	[41.01, 45.85]	p < 0.0001
Education	14.86 (1.31)	12	17	15.43 (2.18)	12	18	0.57	[-0.56, 1.70]	p = 0.32
MMSE	29.62 (0.59)	28	30	29.19 (0.87)	28	30	-0.43	[-0.89, 0.04]	p = 0.07
CES-D score	5.38 (3.64)	0	14	4.71 (4.22)	0	13	-0.67	[-3.13, 1.79]	p = 0.58
Ishihara color blindness	13.52 (2.18)	4	14	14.00 (0.00)	14	14	0.48	[-0.52, 1.47]	p = 0.32
Contrast sensitivity*	1.83 (0.07)	1.72	2.00	1.72 (0.08)	1.48	1.80	-0.10	[-0.15, -0.06]	p < 0.0001
Speed test (s)*	56.57 (4.73)	48	73	63.90 (15.30)	50	120	7.33	[0.24, 14.43]	p < 0.04
No. of attempts in practice vMWM	2.86 (1.06)	1	5	3.57 (1.29)	2	6	0.71	[-0.02, 1.45]	p = 0.06

Legend: Min. = minimum; Max. = maximum; CI = confidence interval; Education = education of participant in years; MMSE = Mini-Mental State Examination; CES-D = Center for Epidemiological Studies Depression scale; No. = number; vMWM = virtual Morris water maze.
*Significant age group differences ($p < 0.05$)

Table 2: Demographics and Test Results for Two Subgroups of Older Adults Divided by the Median of Their Average Corrected Cumulative Proximity in A1 Place Trials

	Older Good Performers (n = 11)			Older Poor Performers (n=10)			
Demographic or pretest variable	M (SD)	Min.	Max.	M (SD)	Min.	Max.	p-value
Age	66.27 (3.55)	60	70	65.10 (5.10)	60	79	p = 0.55
Education	15.27 (2.00)	12	18	15.60 (2.46)	12	18	p = 0.74
MMSE	29.45 (0.82)	28	30	28.90 (0.88)	28	30	p = 0.15
CES-D score	5.36 (5.18)	0	13	4.00 (2.94)	0	9	p = 0.47
Ishihara color blindness	14.00 (0.00)	14	14	14.00 (0.00)	14	14	N/A
Contrast sensitivity	1.72 (0.06)	1.60	1.80	1.72 (0.09)	1.48	1.80	p = 1.00
Speed test (s)	64.91 (18.79)	55	120	62.80 (10.35)	50	80	p = 0.76
No. of attempts in practice vMWM	3.36 (1.12)	2	6	3.65 (1.48)	2	6	p = 0.62

Legend: Min. = minimum; Max. = maximum; CI = confidence interval; Education = education of participant in years; MMSE = Mini-Mental State Examination; CES-D = Center for Epidemiological Studies Depression scale; No. = number; vMWM = virtual Morris water maze.

Table 3: Demographics and Test Results for Two Subgroups of Older Adults Divided by the Median of Their Average Corrected Cumulative Proximity in A2 & A3 Place Trials

	Older Good Performers (n = 11)			Older Poor Performers (n=10)			
Demographic or pretest variable	M (SD)	Min.	Max.	M (SD)	Min.	Max.	p-value
Age	66.00 (3.52)	60	70	65.40 (5.58)	60	79	p = 0.77
Education	15.73 (2.28)	12	18	15.10 (2.13)	12	18	p = 0.52
MMSE	29.36 (0.81)	28	30	29.00 (0.94)	28	30	p = 0.36
CES-D score	5.36 (4.25)	0	11	4.00 (4.29)	0	13	p = 0.47
Ishihara color blindness	14.00 (0.00)	14	14	14.00 (0.00)	14	14	N/A
Contrast sensitivity	1.74 (0.06)	1.60	1.80	1.70 (0.09)	1.48	1.80	p = 0.24
Speed test (s)	59.09 (4.28)	55	70	69.20 (20.55)	50	120	p = 0.13
No. of attempts in practice vMWM*	3.00 (0.77)	2	4	4.20 (1.48)	2	6	p = 0.03

Legend: Min. = minimum; Max. = maximum; CI = confidence interval; Education = education of participant in years; MMSE = Mini-Mental State Examination; CES-D = Center for Epidemiological Studies Depression scale; No. = number; vMWM = virtual Morris water maze. *Significant group difference ($p < 0.05$)

3.2 vMWM Performance

3.2.1 A1 Place Trials

Corrected cumulative proximity was used to measure performance in place trials of the vMWM. CCProx values were averaged across blocks of four trials, as in previous studies (e.g., Driscoll *et al.*, 2005; Gallagher *et al.*, 1993; Magnusson *et al.*, 2007). Age differences in vMWM place trial performance outside of the scanner were assessed using a mixed-model ANCOVA with age groups (young, old-good performers, and old-poor performers) and 6 blocks of 4 hidden trials as the independent variables and corrected cumulative proximity as the dependent variable. After controlling for covariate effect of mean visible pathlength based on A1 control trials ($p = 0.014$), there were significant effects of performance group ($p < 0.001$) and trial ($p = 0.019$) and a significant Group x Trial interaction ($p = 0.006$) (sphericity assumed) (Fig. 3A).

Post hoc Bonferroni comparisons showed that the poor-performing older group had significantly higher (worse-performing) CCProx values than the younger and good-performing older adults ($p < 0.001$) in trials outside the scanner (Fig. 3A). These performance differences were due to significant differences in trial blocks 2-5 for good-performing vs. poor-performing older adults and in trial blocks 2-6 for younger vs. poor-performing older adults ($p < 0.004$, post hoc independent *t*-tests; Fig. 3A). Young adults demonstrated continuous decreases in corrected cumulative proximity across trial blocks ($p < 0.001$), showing steady improvements in search performance. Older good performers appear to show improved search accuracy between the first and second trial blocks, and their learning across trial blocks approached significance ($p = 0.058$). The poor-performing older adults showed little improvement across trials ($p = 0.974$).

To make sure that these performance differences based on a median performance split of older participants were an effect of age, the young participants were divided by their median performance (median = 93.03) and the mixed-model ANCOVA was repeated using four groups: good- and poor-performing older adults and good- and poor-performing younger adults. In this analysis there were significant main effects of group ($p < 0.001$) and trial ($p = 0.003$) and a significant Group x Trial interaction ($p = 0.005$) as before. Post hoc Bonferroni comparisons showed no significant difference in task performance between good- and poor-performing younger adults nor between either younger group and good-performing older adults. The poor-performing older group had significantly worse task performance than both younger groups ($ps < 0.001$).

3.2.2 A1 Probe Trials

A mixed-model ANCOVA was used to analyze performance of the same three groups across the three platform-absent probe trials. Mean visible pathlength from A1 visible trials was once again used as a covariate. There were significant main effects of age group ($p < 0.031$) and trial ($p < 0.001$), and the Group x Trial interaction was not significant ($p = 0.346$) (sphericity assumed) (Fig. 3B). Post hoc Bonferroni comparisons showed that the older poor performers displayed significantly higher average proximity values than the younger adults ($p = 0.024$) but not the older good performers ($p = 0.264$). There was no significant difference in performance between the good-performing older adults and the young. All three groups had significantly lower average proximity values in the second and third trials compared to the first (naïve) probe trial ($ps < 0.001$), showing a learning effect across trials.

3.2.3 A2 & A3 Place Trials

A mixed-model ANCOVA was used to analyze performance of the young and two older subgroups across five blocks of four trials completed in the mock and fMRI scanners. Mean visible pathlength from visible trials in A2 and A3 was used as a covariate. These place trials were analyzed separately from out-of-scanner place trials because the task conditions changed slightly: each place trial was limited to 30s in the scanners (compared to 60s outside the scanners), and participants were told before entering the scanners that the platform would be stationary in all future place trials. In addition, the good- and poor-performing older groups in this analysis are split based on median performance across A2 and A3 place trials instead of A1 trials. There were significant main effects of age ($p = 0.029$) and trial ($p = 0.022$) and a non-

significant Group x Trial interaction (p = 0.864) (sphericity assumed) (Fig. 3C). Post hoc Bonferroni pairwise comparisons showed that the younger group still outperformed the older poor-performing participants but to a lesser extent than in A1 (p = 0.025). The older poor performers did not do significantly worse than the older good performers (p = 0.208).

3.2.4 Visible Trials

A mixed-model ANCOVA was used to analyze performance of the three subgroups (divided by an A1-based median split) across all 20 visible control trials completed in A1, A2, and A3. Self-reported computer experience was used as a covariate. There were significant main effects of age (p = 0.044) and trial (p < 0.001) and a significant Group x Trial interaction (p < 0.001) (sphericity assumed) (Fig. 3D). Post hoc Bonferroni comparisons showed that the poor-performing older adults had significantly higher corrected cumulative proximity overall than the younger adults (p = 0.045) but not the older good performers (p = 0.210).

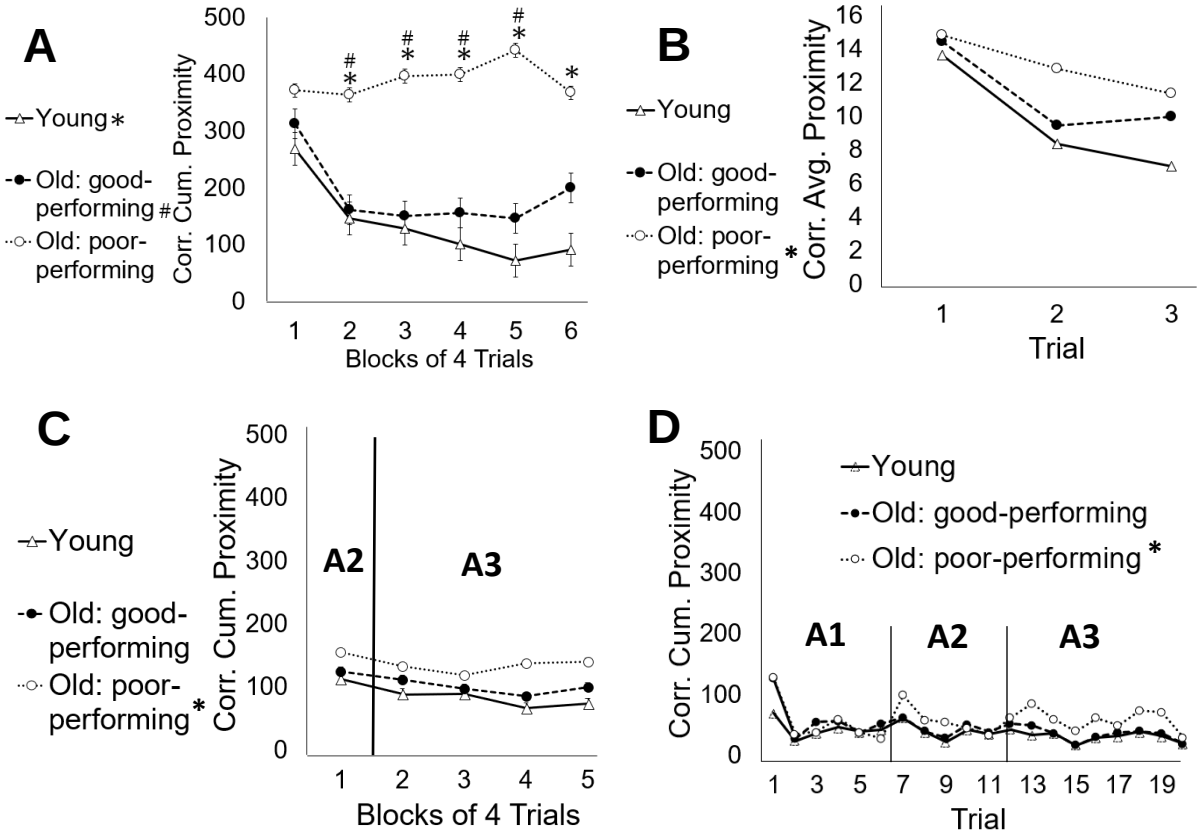

Figure 3: Performance of young participants, good older performers, and poor older performers in the vMWM in place trials outside the scanner (A), place trials within the mock scanner (B: A2) and scanner (B: A3), probe trials outside the scanner (C), and visible trials outside the scanner (D: A1), within the mock scanner (D: A2) and scanner (D: A3). Symbols indicate p < 0.05 for difference from young (*) or good-performing older adults (#).
Corr. Cum. Proximity = Corrected Cumulative Proximity. Corr. Avg. Proximity = Corrected Average Proximity. Lines denote transitions between testing phases (A1, A2, and A3).

3.3 Brain activations

First, brain activation patterns were examined in younger and older participants during place trials in the vMWM compared to control trials (Tables 4-5). We found significant clusters of activation for both groups in the inferior middle gyrus bilaterally (BA 47) and left middle frontal gyrus (BA 9/10 in older, BA 6 in young). Both groups also had activations in the medial frontal gyrus (BA 8) and superior occipital gyrus (BA 19), though in different hemispheres. Only older adults had significant activations in the precuneus (BA 31) and cuneus (BA 18), while only younger adults displayed activations in the cerebellum, caudate, thalamus, and middle occipital gyrus (BA 18).

Table 4: Activations in older adults during spatial navigation in the vMWM compared to control condition

Region	**Side**	**BA**	**Cluster size (voxels)**	**x**	**y**	**z**	***T*-value**
Precuneus	R	31	5370	20	-58	24	8.04
Inferior frontal gyrus	R	47	3196	34	30	0	6.95
	L	47	956	-32	28	2	7.48
Middle frontal gyrus	L	9	2910	-46	32	28	7.70
	L	10	340	-38	58	8	5.57
Superior occipital gyrus	R	19	389	34	-82	30	5.27
Cuneus	R	18	222	10	-88	20	4.39
Medial frontal gyrus	L	8	188	-6	28	48	4.16

Legend: R = Right, L = Left

Table 5: Activations in younger adults during spatial navigation in the vMWM compared to control condition

Region	**Side**	**BA**	**Cluster size (voxels)**	**x**	**y**	**z**	***T*-value**
Superior occipital gyrus	L	19	9093	-32	-84	30	8.85
Cerebellum (posterior lobe)	L		5290	-14	-42	-42	6.61
Frontal lobe (sub-gyral)	L	6	2266	26	0	54	7.37
Middle frontal gyrus	L	6	1038	-36	-2	52	6.31
Inferior frontal gyrus	R	47	967	36	28	0	8.39
	L	47	710	-30	30	0	7.42
Medial frontal gyrus	R	8	494	10	18	50	4.3
Middle occipital gyrus	R	18	475	14	-98	14	6.52
Caudate head	R		320	10	6	2	4.98
Pulvinar	R		134	2	-32	-2	4.9

Legend: R = Right, L = Left

Differences in brain activity between young, good-performing older, and poor-performing older adults were assessed during a well-learned phase of the vMWM to investigate differences in underlying spatial memory-related brain response. One poor-performing older subject who exhibited excessive head motion was removed from fMRI data analysis. Independent samples *t*-tests were performed on percent BOLD signal change for the Hidden Trial – Visible Trial contrast for the following comparisons: Older vs. Young Adults, Good-performing older Adults vs. Young Adults, Poor-performing older Adults vs. Young Adults, and Good-performing older Adults vs. Poor-performing older Adults (Table 6).

Younger subjects showed greater activation in the cerebellum compared to all older adults as well as both older subgroups, and older good performers also showed greater activity in this region than older poor performers (Fig. 4). Older participants overall had decreased activity in the middle occipital gyrus (BA 18) compared to the young which may be due to decreased activity specifically in the older poor performers. Young subjects had greater activity in the parahippocampal gyrus (BA 30) in both hemispheres than older good performers and greater activity in the inferior temporal gyrus (BA 37) than older poor performers. Finally, older good performers displayed greater activations in the middle frontal gyrus (BA 11), superior frontal gyrus (BA 10), and cuneus (BA 18) compared to older poor performers.

Table 6: Between-group differences in brain activations during a well-learned phase of the vMWM

Young > Older

Region	**Side**	**BA**	**Cluster size (voxels)**	**x**	**y**	**z**	***T*-value**
Cerebellum (anterior lobe)	R		1661	6	-68	-10	5.34
Middle occipital gyrus	R	18	370	14	-98	14	4.75
Cerebellum (posterior lobe)	R		263	44	-62	-32	3.56

Young > Older good performers

Region	**Side**	**BA**	**Cluster size (voxels)**	**x**	**y**	**z**	***T*-value**
Cerebellum (anterior lobe)	L		734	0	-60	-4	4.59
Parahippocampal gyrus	R	30	156	30	-48	4	4.40
Parahippocampal gyrus	L	30	152	-28	-56	6	4.83

Young > Older poor performers

Region	**Side**	**BA**	**Cluster size (voxels)**	**x**	**y**	**z**	***T*-value**
Cerebellum (anterior lobe)	L		1839	-4	-44	-16	6.10
Middle occipital gyrus	R	18	402	14	-98	14	4.35
Inferior temporal gyrus	R	37	133	44	-66	0	4.41

Older good performers > Older poor performers

Region	**Side**	**BA**	**Cluster size (voxels)**	**x**	**y**	**z**	***T*-value**
Middle frontal gyrus	L	11	763	-20	48	-12	10.59
Superior frontal gyrus	R	10	262	24	58	4	6.65
Cuneus	L	18	243	0	-102	6	5.22
Cerebellum (posterior lobe)	R		229	14	-88	-30	6.31

Legend: R = Right, L = Left

(a) Young > Older good performers

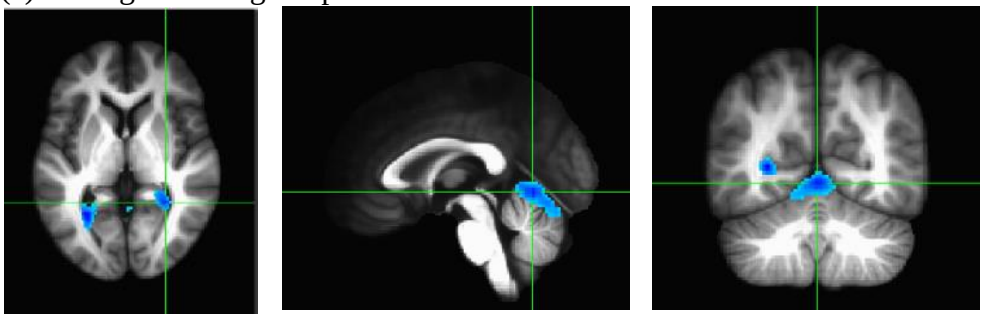

(b) Young > Older poor performers

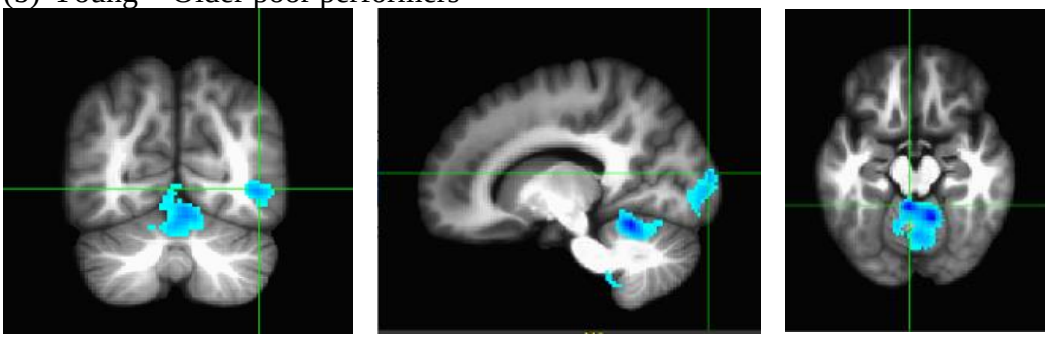

(c) Older good performers > Older poor performers

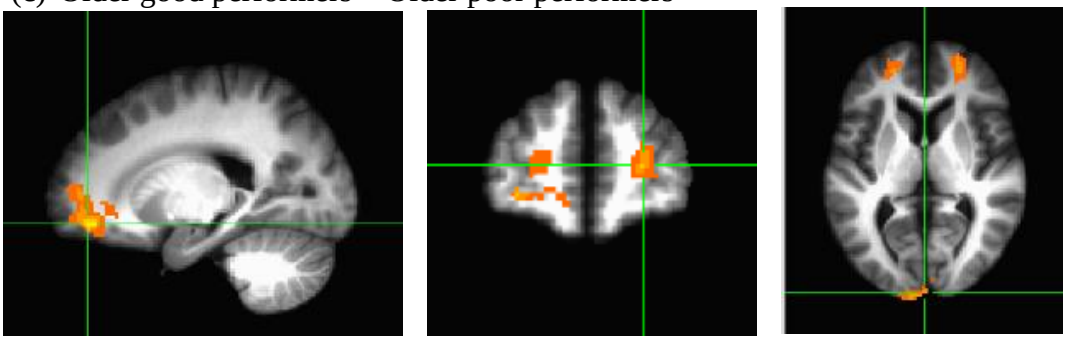

Figure 4: Group comparisons of young, good-performing older, and poor-performing older adults during place trials compared to control trials.

(a) Activations that were greater in younger versus older good performers included the parahippocampal gyrus and the cerebellum.
(b) Activations that were greater in younger than older poor performers included the cerebellum, middle occipital gyrus, and inferior temporal gyrus.
(c) Brain activations that were greater in older good than older poor performers included the middle frontal gyrus, superior frontal gyrus, and cuneus.

4. DISCUSSION

This study evaluated age-related differences in human spatial learning using a virtual water maze task in conjunction with fMRI to characterize differences in brain activity between older good performers, older poor performers, and young adults. Corrected cumulative proximity was used as a measure of performance in the vMWM, which was designed based on MWM protocols previously used in mouse studies (Magnusson, 1998; Magnusson et al., 2007, Zhao et al., 2009). The behavioral results of the current study demonstrated that some older adults struggled to form spatial memories in a new environment compared to younger adults, while others performed comparably to younger adults. Telling participants that the platform was stationary reduced the performance deficit of older poor performers in a well-learned phase of the vMWM, but a significant performance shortfall remained compared to young participants.

Overall, younger adults demonstrated greater activity than all older participants in the cerebellum. This increased activity was also observed in the young compared to older good performers and older poor performers as well as in older good performers compared to older poor performers. The cerebellum supports motor coordination and hand-eye coordination and may show greater activity in younger participants because the older group had more difficulty navigating with a joystick (Miall et al., 2001). Underactivation of the cerebellum in older participants, particularly among the poor performers, could also be explained by age-related shrinkage in cerebellum volume (Moffat et al., 2007). The cerebellum has been shown to have a strong involvement in spatial navigation by maintaining a perception of direction and location during motion and participating in somatosensory integration (Rondi-Reig et al., 2014). By continuously providing self-motion information to an updating hippocampal spatial map, potentially via the posterior parietal and retrosplenial cortices, the cerebellum has been proposed to be part of the spatial navigation network (Rochefort et al., 2013).

Younger adults also demonstrated greater activity in the parahippocampal gyrus compared to good-performing older adults during a well-rehearsed portion of the vMWM. Neuroimaging studies have shown that parahippocampal activity during navigational tasks was lower (Meulenbroek et al., 2004; Moffat et al., 2006) or absent (Antonova et al., 2009) in non-demented older adults compared to younger adults. Activation in the parahippocampal gyrus has been associated with the encoding of navigationally relevant landmarks and their spatial positions (Aguirre et al., 1996; Maguire et al., 1998; Bohbot et al., 2015). Janzen et al. (2004, 2011) found that the parahippocampal gyrus shows greater activity in response to landmarks located at decision points than those found at non-decision points, indicating that this region may play a role in distinguishing between navigationally relevant and irrelevant objects.

Of interest was the finding that older good performers displayed greater activations in prefrontal regions in both hemispheres, specifically the middle (BA 11) and superior frontal gyrus (BA 10). These two Brodmann areas overlap with the medial prefrontal cortex (mPFC) and orbitofrontal cortex (OFC) (Rogers et al., 1999; Bechara, 2004; Frey & Petrides, 2000; Kringelbach & Rolls, 2004; Ongur et al., 2003; Ramnani & Own, 2004). The hippocampus is critical to spatial memory formation, but with time, spatial memories become more dependent on extrahippocampal regions (Teng & Squire, 1999; Rosenbaum et al., 2000). During memory consolidation, hippocampus-dependent spatial memories become stored in the cortex as they

mature (Marr, 1971; McClelland et al., 1995; Squire & Alvarez, 1995; Wiltgen et al., 2004; Frankland & Bontempi, 2005; Smith & Squire, 2009), including the frontal cortex.

There is considerable evidence that the mPFC facilitates short-term and long-term learning and memory consolidation over a wide range of cognitive tasks (Euston et al., 2012, Leon et al., 2010, Tronel & Sara, 2003). In fact, it has been proposed that the medial PFC is essential for the stabilization of recently acquired memories (Euston et al., 2012; Carballo-Marquez, 2007; Tronel et al., 2004; Izaki et al., 2000, Carballo-Marquez et al., 2009; Akirav & Maroun, 2006), including those formed while completing the Morris water maze (Leon et al., 2010) as well as the retrieval of remote memories (Bontempi et al., 1999, Frankland et al., 2004, Takashima et al., 2006). Euston *et al.* (2012) has proposed that the function of the mPFC is to "learn associations between context, locations, events, and corresponding adaptive responses." Slotnick & Moo (2006) found that the left mPFC (BA10) preferentially processes categorical visual spatial memory including source memory while the right mPFC (BA9/10) is preferentially associated with coordinate visual spatial memory.

The mPFC has also been shown to be heavily involved in the acquisition, consolidation, and retrieval of hippocampus-dependent spatial memories. Hok *et al.* (2005) demonstrated that neuronal firing in the mPFC corresponds to the motivational salience of places in rats conducting a place navigation task. They proposed that this spatio-selective activity in the mPFC might encode goals that are necessary for path planning. Conversely, damaging the ventral and intermediate hippocampus disrupted mPFC goal firing (Burton et al., 2009) and behavioral performance (Wang & Cai, 2006) in a place navigation task. Kyd & Bilkey (2003) found evidence that hippocampal place cell activity changes after large mPFC lesions occur, indicating that dynamic interactions exist between the hippocampus and the mPFC. mPFC lesions also make hippocampal place fields less stable over time and more susceptible to changes in an individuals' local environment (Kyd & Bilkey, 2005).

Hok et al. (2013) found that post-training inactivation of PFC of rodents doing a place navigation task does not affect behavioral performance, suggesting that the mPFC is no longer required for a navigation task when animals are well-trained. Similarly, Lee & Kesner (2003) suggested that the mPFC was no longer required to complete a spatial working memory task with an intermediate- or long-term delayed response when the rules were simplified. This group also demonstrated that inactivating either the mPFC or the dorsal hippocampus in rats generated an initial impairment in short-term spatial working memory that returned to normal levels of performance over time, suggesting that compensatory adjustments may occur between these two regions that work together to process spatial memory.

The medial PFC has also been demonstrated to be involved in other skills besides memory that are necessary for completing the vMWM, including decision making (Botnivnick et al., 2004), executive control (Posner et al., 2007), and reward-guided learning (Rushworth et al., 2011). Specifically, this region processes representations of goals as well as rules and strategies during a task (Owen & Verberne, 1996; Robbins, 2000; Gaffan, 2002; Rushworth et al., 2002; Brass et al., 2003), and this active maintenance affects stimulus-response mappings in other regions (Miller & Cohen, 2001). There is evidence that value and reward signals from the orbital and medial PFC and striatum are processed in the lateral PFC to guide action selection, and this

system has a sensitivity to abstractness that allows for both strategically selected and self-controlled pursuit of goal-directed action (Coutlee & Huettel, 2012).

The orbitofrontal cortex plays a similar role to the medial PFC; it has even been proposed that the two regions functionally be referred to collectively as the orbitomedial cortex. PET imaging has shown that he orbitofrontal cortex (BA 11) is crucial for encoding new information for memory processing (Frey & Petrides, 2000). Additionally, Domenech & Koechlin proposed a model based on neuroimaging evidence that the PFC consists of two functions: a peripheral system including the OFC that is involved in choosing actions based on perceptual cues and reward values and a core system including the mPFC that is involved in adaptive behavior in variable environments and probabilistic reasoning (2015). Furthermore, Wikenheiser & Schoenbaum (2016) present evidence that the hippocampus and OFC encode parallel cognitive maps of cues, environmental features, actions, and outcomes to allow goal-directed decision making.

Limitations & Future Directions

One key difference between the traditional rodent MWM and the vMWM used with humans is the issue of motivation. Rodents are rewarded when they reach the hidden platform by being raised up out of uncomfortably cold water, while human participants were motivated to reach the hidden platform only because they were instructed to do so. Future vMWM studies should also try to address age-related differences in hand-eye coordination by creating new handheld devices to facilitate virtual navigation such as a small driving wheel. In assessing spatial learning ability in the vMWM, due to heterogeneity in cognitive aging, only longitudinal studies will be able to determine if older adults showing greater cognitive difficulties have experienced a greater lifetime cognitive decline than their good-performing counterparts.

To our knowledge, this study is the first to use a cumulative proximity measure to assess water maze navigation in humans using an experimental protocol adapted from spatial memory research that used rodent models. We expect this study to confirm the relevance of a mouse model of brain region recruitment by older individuals, allowing more invasive techniques to be used to further investigate the phenomenon such as electrophysiology and gene silencing. We are currently investigating brain activations in older versus younger subjects during the early learning phase of virtual water maze learning. In the future, it could be useful to see what regions are activated in older poor performers compared to older good performers and younger subjects during the plateaued performance phase observed during A1. Additionally, we believe that this virtual water maze could be used to assess the efficacy of interventions into cognitive aging in both humans and rodents, enabling us to better perform both mechanistic and translational aging research.

5. ACKNOWLEDGEMENTS

Thank you to support provided by NIH grant K18 AG048706 and CVM Pilot Project funds to Dr. Magnusson and by Oregon State University URSA-Engage and Life Scholars funds to me. Special thanks to Jimmy Zhong, Dr. Scott Moffat, Cherita Clendinen, and Dr. Matthew Swarts from Georgia Institute of Technology for their extensive work on this project. Thank you also to Dr. Fikru Nigussie and Dr. Anita Cservenka for their support as committee members. Finally, I extend my sincere gratitude to Dr. Kathy Magnusson for her mentorship and guidance throughout this adventure.

6. REFERENCES

Aguirre, G. K. & D'Esposito, M. Environmental knowledge is subserved by separable dorsal/ventral neural areas. *J. Neurosci.* **17,** 2512–2518 (1997).

Akirav, I. & Maroun, M. Ventromedial prefrontal cortex is obligatory for consolidation and reconsolidation of object recognition memory. *Cereb. Cortex* **16,** 1759–1765 (2006).

Andersson, J. L., Hutton, C., Ashburner, J., Turner, R. & Friston, K. Modeling geometric deformations in EPI time series. *Neuroimage* **13,** 903–919 (2001).

Antonova, E. *et al.* Age-related neural activity during allocentric spatial memory. *Memory* **17,** 125–143 (2009).

Astur, R. S., Ortiz, M. L. & Sutherland, R. J. A characterization of performance by men and women in a virtual Morris water task: a large and reliable sex difference. *Behav. Brain Res.* **93,** 185–190 (1998).

Bechara, A. Disturbances of Emotion Regulation After Focal Brain Lesions. in *International Review of Neurobiology* **62,** 159–193 (Academic Press, 2004).

Begega, A. *et al.* Effects of ageing on allocentric and egocentric spatial strategies in the Wistar rat. *Behavioural Processes* **53,** 75–85 (2001).

Benke, T., Karner, E., Petermichl, S., Prantner, V. & Kemmler, G. Neuropsychological deficits associated with route learning in Alzheimer disease, MCI, and normal aging. *Alzheimer Dis Assoc Disord* **28,** 162–167 (2014).

Bohbot, V. D. *et al.* Role of the parahippocampal cortex in memory for the configuration but not the identity of objects: converging evidence from patients with selective thermal lesions and fMRI. *Front. Hum. Neurosci.* **9,** (2015).

Bontempi, B., Laurent-Demir, C., Destrade, C. & Jaffard, R. Time-dependent reorganization of brain circuitry underlying long-term memory storage. *Nature* **400,** 671–675 (1999).

Botvinick, M. M., Cohen, J. D. & Carter, C. S. Conflict monitoring and anterior cingulate cortex: an update. *Trends Cogn. Sci. (Regul. Ed.)* **8,** 539–546 (2004).

Brass, M., Derrfuss, J., Matthes-von Cramon, G. & von Cramon, D. Y. Imitative response tendencies in patients with frontal brain lesions. *Neuropsychology* **17,** 265–271 (2003).

Burton, B. G., Hok, V., Save, E. & Poucet, B. Lesion of the ventral and intermediate hippocampus abolishes anticipatory activity in the medial prefrontal cortex of the rat. *Behav. Brain Res.* **199,** 222–234 (2009).

Cabeza, R. Cognitive neuroscience of aging: Contributions of functional neuroimaging. *Scandinavian Journal of Psychology* **42,** 277–286 (2001).

Carballo-Márquez, A. *et al.* Differential effects of muscarinic receptor blockade in prelimbic cortex on acquisition and memory formation of an odor-reward task. *Learn. Mem.* **14,** 616–624 (2007).

Carballo-Márquez, A., Vale-Martínez, A., Guillazo-Blanch, G. & Martí-Nicolovius, M. Muscarinic receptor blockade in ventral hippocampus and prelimbic cortex impairs memory for socially transmitted food preference. *Hippocampus* **19,** 446–455 (2009).

Coutlee, C. G. & Huettel, S. A. The Functional Neuroanatomy of Decision Making: Prefrontal Control of Thought and Action. *Brain Res* **1428C,** 3–12 (2012).

Daugherty, A. M. *et al.* Path Complexity in Virtual Water Maze Navigation: Differential Associations with Age, Sex, and Regional Brain Volume. *Cereb Cortex* **25,** 3122–3131 (2015).

Domenech, P. & Koechlin, E. Executive control and decision-making in the prefrontal cortex. *Current Opinion in Behavioral Sciences* **1,** 101–106 (2015).

Driscoll, I. *et al.* The aging hippocampus: cognitive, biochemical and structural findings. *Cereb. Cortex* **13,** 1344–1351 (2003).

Driscoll, I., Hamilton, D. A., Yeo, R. A., Brooks, W. M. & Sutherland, R. J. Virtual navigation in humans: the impact of age, sex, and hormones on place learning. *Horm Behav* **47,** 326–335 (2005).

Euston, D. R., Gruber, A. J. & McNaughton, B. L. The Role of Medial Prefrontal Cortex in Memory and Decision Making. *Neuron* **76,** 1057–1070 (2012).

Frankland, P. W., Bontempi, B., Talton, L. E., Kaczmarek, L. & Silva, A. J. The involvement of the anterior cingulate cortex in remote contextual fear memory. *Science* **304,** 881–883 (2004).

Frey, S. & Petrides, M. Orbitofrontal cortex: A key prefrontal region for encoding information. *Proc Natl Acad Sci U S A* **97,** 8723–8727 (2000).

Gallagher, M., Burwell, R. & Burchinal, M. Severity of spatial learning impairment in aging: development of a learning index for performance in the Morris water maze. *Behav. Neurosci.* **107,** 618–626 (1993).

Gallagher, M. & Pelleymounter, M. A. Spatial learning deficits in old rats: A model for memory decline in the aged. *Neurobiology of Aging* **9,** 549–556 (1988).

Genovesio, A., Brasted, P. J. & Wise, S. P. Representation of Future and Previous Spatial Goals by Separate Neural Populations in Prefrontal Cortex. *J Neurosci* **26,** 7305–7316 (2006).

Genovesio, A., Tsujimoto, S. & Wise, S. P. Encoding problem-solving strategies in prefrontal cortex: Activity during strategic errors. *Eur J Neurosci* **27,** 984–990 (2008).

Gillner, S. & Mallot, H. A. Navigation and Acquisition of Spatial Knowledge in a Virtual Maze. *Journal of Cognitive Neuroscience* **10,** 445–463 (1998).

Grön, G., Wunderlich, A. P., Spitzer, M., Tomczak, R. & Riepe, M. W. Brain activation during human navigation: gender-different neural networks as substrate of performance. *Nat. Neurosci.* **3,** 404–408 (2000).

Hok, V., Save, E., Lenck-Santini, P. P. & Poucet, B. Coding for spatial goals in the prelimbic/infralimbic area of the rat frontal cortex. *PNAS* **102,** 4602–4607 (2005).

Hok, V., Chah, E., Save, E. & Poucet, B. Prefrontal cortex focally modulates hippocampal place cell firing patterns. *J. Neurosci.* **33,** 3443–3451 (2013).

Höller-Wallscheid, M. S., Thier, P., Pomper, J. K. & Lindner, A. Bilateral recruitment of prefrontal cortex in working memory is associated with task demand but not with age. *Proceedings of the National Academy of Sciences of the United States of America* **114,** E830–E839 (2017).

Iacobucci, D., Posavac, S. S., Kardes, F. R., Schneider, M. J. & Popovich, D. L. The median split: Robust, refined, and revived. *Journal of Consumer Psychology* **25,** 690–704 (2015).

Izaki, Y., Hori, K. & Nomura, M. Disturbance of rat lever-press learning by hippocampo-prefrontal disconnection. *Brain Res.* **860,** 199–202 (2000).

Janzen, G. & van Turennout, M. Selective neural representation of objects relevant for navigation. *Nat. Neurosci.* **7,** 673–677 (2004).

Jo, Y. S. *et al.* The medial prefrontal cortex is involved in spatial memory retrieval under partial-cue conditions. *J. Neurosci.* **27,** 13567–13578 (2007).

Jones, M. W. & Wilson, M. A. Theta Rhythms Coordinate Hippocampal–Prefrontal Interactions in a Spatial Memory Task. *PLoS Biol* **3,** (2005).

Kessels, R. P. C., Postma, A., Wijnalda, E. M. & Haan, E. H. F. de. Frontal-Lobe Involvement in Spatial Memory: Evidence from PET, fMRI, and Lesion Studies. *Neuropsychol Rev* **10,** 101–113 (2000).

Knierim, J. J., Kudrimoti, H. S. & McNaughton, B. L. Place cells, head direction cells, and the learning of landmark stability. *J. Neurosci.* **15,** 1648–1659 (1995).

Kringelbach, M. L. & Rolls, E. T. The functional neuroanatomy of the human orbitofrontal cortex: evidence from neuroimaging and neuropsychology. *Progress in Neurobiology* **72,** 341–372 (2004).

Kyd, R. J. & Bilkey, D. K. Prefrontal cortex lesions modify the spatial properties of hippocampal place cells. *Cereb. Cortex* **13,** 444–451 (2003).

Kyd, R. J. & Bilkey, D. K. Hippocampal place cells show increased sensitivity to changes in the local environment following prefrontal cortex lesions. *Cereb. Cortex* **15,** 720–731 (2005).

Laurance, H. E. *et al.* Older Adults Map Novel Environments but Do Not Place Learn: Findings from a Computerized Spatial Task. *Aging, Neuropsychology, and Cognition* **9,** 85–97 (2002).

Lee, I. & Kesner, R. P. Time-Dependent Relationship between the Dorsal Hippocampus and the Prefrontal Cortex in Spatial Memory. *J. Neurosci.* **23,** 1517–1523 (2003).

Leon, W. C., Bruno, M. A., Allard, S., Nader, K. & Cuello, A. C. Engagement of the PFC in consolidation and recall of recent spatial memory. *Learn. Mem.* **17,** 297–305 (2010).

Lindner, M. D., Plone, M. A., Schallert, T. & Emerich, D. F. Blind rats are not profoundly impaired in the reference memory Morris water maze and cannot be clearly discriminated from rats with cognitive deficits in the cued platform task. *Cognitive Brain Research* **5,** 329–333 (1997).

Lithfous, S., Dufour, A. & Després, O. Spatial navigation in normal aging and the prodromal stage of Alzheimer's disease: insights from imaging and behavioral studies. *Ageing Res. Rev.* **12,** 201–213 (2013).

Lukoyanov, N. V., Andrade, J. P., Dulce Madeira, M. & Paula-Barbosa, M. M. Effects of age and sex on the water maze performance and hippocampal cholinergic fibers in rats. *Neuroscience Letters* **269,** 141–144 (1999).

Maei, H. R., Zaslavsky, K., Teixeira, C. M. & Frankland, P. W. What is the Most Sensitive Measure of Water Maze Probe Test Performance? *Front Integr Neurosci* **3,** (2009).

Magnusson, K. R. Aging of glutamate receptors: correlations between binding and spatial memory performance in mice. *Mech. Ageing Dev.* **104,** 227–248 (1998).

Magnusson, K. R., Scruggs, B., Zhao, X. & Hammersmark, R. Age-related declines in a two-day reference memory task are associated with changes in NMDA receptor subunits in mice. *BMC Neurosci* **8,** 43 (2007).

Maguire, E. A., Frith, C. D., Burgess, N., Donnett, J. G. & O'Keefe, J. Knowing where things are parahippocampal involvement in encoding object locations in virtual large-scale space. *J Cogn Neurosci* **10,** 61–76 (1998).

Marr, D. Simple memory: a theory for archicortex. *Phil. Trans. R. Soc. Lond. B* **262,** 23–81 (1971).

Martinet, L.-E., Sheynikhovich, D., Benchenane, K. & Arleo, A. Spatial Learning and Action Planning in a Prefrontal Cortical Network Model. *PLOS Computational Biology* **7,** e1002045 (2011).

McClelland, J. L., McNaughton, B. L. & O'Reilly, R. C. Why there are complementary learning systems in the hippocampus and neocortex: insights from the successes and failures of connectionist models of learning and memory. *Psychol Rev* **102,** 419–457 (1995).

Meulenbroek, O., Petersson, K. M., Voermans, N., Weber, B. & Fernández, G. Age differences in neural correlates of route encoding and route recognition. *Neuroimage* **22,** 1503–1514 (2004).

Miall, R. C., Reckess, G. Z. & Imamizu, H. The cerebellum coordinates eye and hand tracking movements. *Nat. Neurosci.* **4,** 638–644 (2001).

Miller, E. K. & Cohen, J. D. An integrative theory of prefrontal cortex function. *Annu. Rev. Neurosci.* **24,** 167–202 (2001).

Moffat, S. D., Elkins, W. & Resnick, S. M. Age differences in the neural systems supporting human allocentric spatial navigation. *Neurobiol. Aging* **27,** 965–972 (2006).

Moffat, S. D., Kennedy, K. M., Rodrigue, K. M. & Raz, N. Extrahippocampal contributions to age differences in human spatial navigation. *Cereb. Cortex* **17,** 1274–1282 (2007).

Moffat, S. D. & Resnick, S. M. Effects of Age on Virtual Environment Place Navigation and Allocentric Cognitive Mapping. *Behavioral Neuroscience* **116,** 851–859 (2002).

Moffat, S. D., Zonderman, A. B. & Resnick, S. M. Age differences in spatial memory in a virtual environment navigation task. *Neurobiology of Aging* **22,** 787–796 (2001).

Morris, R. Developments of a water-maze procedure for studying spatial learning in the rat. *J. Neurosci. Methods* **11,** 47–60 (1984).

Morris, R. G. M., Garrud, P., Rawlins, J. N. P. & O'Keefe, J. Place navigation impaired in rats with hippocampal lesions. *Nature* **297,** 681–683 (1982).

Morris, R. G. M. Spatial localization does not require the presence of local cues. *Learning and Motivation* **12,** 239–260 (1981).

Newman, M. C. & Kaszniak, A. W. Spatial memory and aging: Performance on a human analog of the Morris water maze. *Neuropsychology, development, and cognition. Section B, Aging, neuropsychology and cognition* **7,** 86–93 (2000).

Nowak, N. T., Diamond, M. P., Land, S. J. & Moffat, S. D. Contributions of sex, testosterone, and androgen receptor CAG repeat number to virtual Morris water maze performance. *Psychoneuroendocrinology* **41,** 13–22 (2014).

O'Bryant, S. E. *et al.* Detecting dementia with the mini-mental state examination in highly educated individuals. *Arch. Neurol.* **65,** 963–967 (2008).

Oldfield, R. C. The assessment and analysis of handedness: The Edinburgh inventory. *Neuropsychologia* **9,** 97–113 (1971).

Ongür, D., Ferry, A. T. & Price, J. L. Architectonic subdivision of the human orbital and medial prefrontal cortex. *J. Comp. Neurol.* **460,** 425–449 (2003).

Owens, N. C. & Verberne, A. J. M. An electrophysiological study of the medial prefrontal cortical projection to the nucleus of the solitary tract in rat. *Exp Brain Res* **110,** 55–61 (1996).

Parizkova, M. *et al.* The effect of Alzheimer's disease on spatial navigation strategies. *Neurobiology of Aging* **64,** 107–115 (2018).

Posner, M. I., Rothbart, M. K., Sheese, B. E. & Tang, Y. The anterior cingulate gyrus and the mechanism of self-regulation. *Cogn Affect Behav Neurosci* **7,** 391–395 (2007).

Possin, K. L. *et al.* Cross-species translation of the Morris maze for Alzheimer's disease. *J. Clin. Invest.* **126,** 779–783 (2016).

Pratt, W. E. & Mizumori, S. J. Neurons in rat medial prefrontal cortex show anticipatory rate changes to predictable differential rewards in a spatial memory task. *Behav. Brain Res.* **123,** 165–183 (2001).

Preston, A. R. & Eichenbaum, H. Interplay of Hippocampus and Prefrontal Cortex in Memory. *Current Biology* **23,** R764–R773 (2013).

Rahman, Q. & Koerting, J. Sexual orientation-related differences in allocentric spatial memory tasks. *Hippocampus* **18,** 55–63 (2008).

Rahman, Q., Sharp, J., McVeigh, M. & Ho, M.-L. Sexual Orientation-Related Differences in Virtual Spatial Navigation and Spatial Search Strategies. *Arch Sex Behav* **46,** 1279–1294 (2017).

Ramnani, N. & Owen, A. M. Anterior prefrontal cortex: insights into function from anatomy and neuroimaging. *Nature Reviews Neuroscience* **5,** 184–194 (2004).

Robbins, T. W. Chemical neuromodulation of frontal-executive functions in humans and other animals. *Exp Brain Res* **133,** 130–138 (2000).

Rochefort, C., Lefort, J. M. & Rondi-Reig, L. The cerebellum: a new key structure in the navigation system. *Front. Neural Circuits* **7,** (2013).

Rogers, R. D. *et al.* Choosing between Small, Likely Rewards and Large, Unlikely Rewards Activates Inferior and Orbital Prefrontal Cortex. *J. Neurosci.* **19,** 9029–9038 (1999).

Rondi-Reig, L., Paradis, A.-L., Lefort, J. M., Babayan, B. M. & Tobin, C. How the cerebellum may monitor sensory information for spatial representation. *Front. Syst. Neurosci.* **8,** (2014).

Ross, R. S., LoPresti, M. L., Schon, K. & Stern, C. E. Role of the hippocampus and orbitofrontal cortex during the disambiguation of social cues in working memory. *Cogn Affect Behav Neurosci* **13,** (2013).

Rushworth, M. F. S., Hadland, K. A., Paus, T. & Sipila, P. K. Role of the human medial frontal cortex in task switching: a combined fMRI and TMS study. *J. Neurophysiol.* **87,** 2577–2592 (2002).

Rushworth, M. F. S., Noonan, M. P., Boorman, E. D., Walton, M. E. & Behrens, T. E. Frontal cortex and reward-guided learning and decision-making. *Neuron* **70,** 1054–1069 (2011).

Sapiurka, M., Squire, L. R. & Clark, R. E. Distinct roles of hippocampus and medial prefrontal cortex in spatial and nonspatial memory. *Hippocampus* **26,** 1515–1524 (2016).

Schlichting, M. L. & Preston, A. R. Hippocampal-medial prefrontal circuit supports memory updating during learning and post-encoding rest. *Neurobiol Learn Mem* **134,** 91–106 (2016).

Schoenfeld, R., Schiffelholz, T., Beyer, C., Leplow, B. & Foreman, N. Variants of the Morris water maze task to comparatively assess human and rodent place navigation. *Neurobiol Learn Mem* **139,** 117–127 (2017).

Scruggs, B., Magnusson, K.R., Zhao, X. & Hammersmark, R. Age-related declines in a two-day reference memory task are associated with changes in NMDA receptor subunits in mice. *BMC Neuroscience* **8,** 43 (2007).

Slotnick, S. D. & Moo, L. R. Prefrontal cortex hemispheric specialization for categorical and coordinate visual spatial memory. *Neuropsychologia* **44,** 1560–1568 (2006).

Smith, C. N. & Squire, L. R. Medial temporal lobe activity during retrieval of semantic memory is related to the age of the memory. *J. Neurosci.* **29,** 930–938 (2009).

Squire, L. R. & Alvarez, P. Retrograde amnesia and memory consolidation: a neurobiological perspective. *Curr. Opin. Neurobiol.* **5,** 169–177 (1995).

Takashima, A. *et al.* Declarative memory consolidation in humans: a prospective functional magnetic resonance imaging study. *Proc. Natl. Acad. Sci. U.S.A.* **103,** 756–761 (2006).

Teixeira, C. M., Pomedli, S. R., Maei, H. R., Kee, N. & Frankland, P. W. Involvement of the Anterior Cingulate Cortex in the Expression of Remote Spatial Memory. *J. Neurosci.* **26,** 7555–7564 (2006).

Touzani, K., Puthanveettil, S. V. & Kandel, E. R. Consolidation of learning strategies during spatial working memory task requires protein synthesis in the prefrontal cortex. *PNAS* **104,** 5632–5637 (2007).

Tronel, S., Feenstra, M. G. P. & Sara, S. J. Noradrenergic Action in Prefrontal Cortex in the Late Stage of Memory Consolidation. *Learn Mem* **11,** 453–458 (2004).

Tronel, S. & Sara, S. J. Blockade of NMDA Receptors in Prelimbic Cortex Induces an Enduring Amnesia for Odor–Reward Associative Learning. *J. Neurosci.* **23,** 5472–5476 (2003).

van Veen, H. A. H. C., Distler, H. K., Braun, S. J. & Bülthoff, H. H. Navigating through a virtual city: Using virtual reality technology to study human action and perception. *Future Generation Computer Systems* **14,** 231–242 (1998).

Vlček, K. & Laczó, J. Neural correlates of spatial navigation changes in mild cognitive impairment and Alzheimer's disease. *Front Behav Neurosci* **8,** 89 (2014).

Vorhees, C. V. & Williams, M. T. Morris water maze: procedures for assessing spatial and related forms of learning and memory. *Nat Protoc* **1,** 848–858 (2006).

Waller, D., Hunt, E. & Knapp, D. The Transfer of Spatial Knowledge in Virtual Environment Training. *Presence: Teleoperators and Virtual Environments* **7,** 129–143 (1998).

Wegman, J. & Janzen, G. Neural encoding of objects relevant for navigation and resting state correlations with navigational ability. *J Cogn Neurosci* **23,** 3841–3854 (2011).

Wiltgen, B. J., Brown, R. A. M., Talton, L. E. & Silva, A. J. New circuits for old memories: the role of the neocortex in consolidation. *Neuron* **44,** 101–108 (2004).

Wu, J. Q., Peters, G. J., Rittner, P., Cleland, T. A. & Smith, D. M. The hippocampus, medial prefrontal cortex and selective memory retrieval: Evidence from a rodent model of the retrieval-induced forgetting effect. *Hippocampus* **24,** 1070–1080 (2014).

Yoon, T., Okada, J., Jung, M. W. & Kim, J. J. Prefrontal cortex and hippocampus subserve different components of working memory in rats. *Learn Mem* **15,** 97–105 (2008).

Zhao, X., Rosenke, R., Kronemann, D., Brim, B., Das, S.R., Dunah, A.W., & Magnusson, K.R. The effects of aging on N-methyl-D-aspartate receptor subunits in the synaptic membrane and relationships to long-term spatial memory. *Neuroscience* **162,** 933–945 (2009).

Zhong, J. Y., Magnusson, K. R., Swarts, M. E., Clendinen, C. A., Reynolds, N. C., & Moffat, S. D. The application of a rodent-based Morris water maze (MWM) protocol to an investigation of age-related differences in human spatial learning. *Behav Neurosci* **131**, 470–482 (2017).